An EEG based Neural Mass Model of Traumatic Brain Injury and Recovery

Jayant P. Menon
jayantsteps@gmail.com

Renga Aravamudhan
arrajan@gmail.com

Vikram Gupta
v3gupta@ucsd.edu

Abstract

Analysis of brain activity reveals the presence of synchronous oscillations over a range of frequencies. These oscillations can be observed using electro-neurological measurements such as electroencephalogram (EEG), magnetoencephalogram (MEG) or electrocorticogram (ECoG) . Further, these rhythms can traverse different connected parts of the brain forming a "system of rhythms". These systems are analyzed in this paper using a lumped-parameter, interconnected, neural mass models. This model allows the analysis of the dynamics of the neural population in the frontal cortex and their synapses using a few state variables. It is assumed here that the neurons share the inputs and synchronizes their activity. The present work is motivated by a recent paper by Bhattacharya et al who have proposed an adaptation of Ursino's neural mass model for the study of the changes in alpha rhythms during the course of Alzheimer's disease. In that work, the synaptic organization and connectivity in the lumped thalmo-cortico-thalmic model was modified using experimental data. The authors were able to reproduce the slowing of alpha rhythms (8-12 Hz) and decrease in power of these rhythms associated with the Alzheimer's disease. Using this research as the basis, the present work employs a pathophysiologic understanding of traumatic brain injury to create a computational model of traumatic brain injury that recreates the multimodal electroencephalographic changes observed to occur with mild, moderate, and severe traumatic brain injury. The focus is on recreating the observed changes in the alpha and gamma rhythms (30-100Hz) due to traumatic brain injury. Eight coupled neural mass models are used to represent the frontal cortex. Numerical simulations are conducted using a well-known software package. It is shown that the present model accurately reproduces the power spectral density of the normal frontal cortex under white-noise excitation conditions. Three degrees of traumatic brain injuries are then modeled by decreasing the connection strengths in the neural mass model. A comparison of the power spectral densities of the outputs of the normal and injured neural mass models indicates that the present model is capable to reproducing clinically-observed changes due to traumatic brain injuries.

1 Traumatic Brain Injury

1.1 Background

Traumatic brain injury (TBI) is defined as an alteration in brain function or other evidence of brain pathology caused by an external force. (McAllister, 2011)TBI is the leading cause of death in individuals less than 35yrs old. It is a leading cause of neuropsychological dysfunction and disability. Nearly 500,000 people a year in the United States are hospitalized with head trauma. Of these, approximately 70,000 suffer from a long-term

disability and 2,000 remain in a persistent vegetative state, alive but unconscious. The annual cost of treatment for TBI in the United States is estimated to be approximately $25 Billion. (Bruns J, 2003) TB is the leading injury for veterans returning from wars in Iraq and Afghanistan. Since October 2001, over 1.6 million American service members have deployed, between 5-35% have had a concussion. It is estimated that 80% of those injuries are due to blast exposure. Although modern helmet technology has enabled protection from penetrating projectiles that cause focal traumatic injury, it cannot protect against TBI caused by blast waves arising from explosions in the proximity. During blast exposure, large forces can be imparted to entire underlying neural tissues causing both focal and diffuse injuries. (Rigg JL, 2011)

The severity of traumatic brain injury is currently graded based upon the Glascow Coma Scale, it is a15-point scale based upon eye opening, verbal and motor responsiveness to requested commands. Severe traumatic injury (GCS 3-8) results in unconsciousness and is seen after high-energy impacts, such as penetrating gunshot wounds. Moderate injury (GCS 9-12) from moderate energy impacts, such as blast injuries; result in severe impairment of consciousness causing disorientation or confusion. Mild injury (GCS 13-15) from low energy impacts, such as a football tackle, can result in mild confusion and disorientation. (Teasdale G, 1974) All injuries have short-term and long-term consequences and constitute a spectrum of physical injuries that damage different neural elements to various degrees.

1.2 Clinical Consequences of TBI

Severe traumatic brain injury often requires surgical intervention to decompress the brain acutely, placement of a surgically implanted monitor to measure intracranial pressure (Rabenstein, 2008) and sometimes implanting a cerebral microdialysis device for neurochemical monitoring (Tisdall MM, 2006). Moderate TBI requires hospitalization in an intensive care setting and occasionally requires invasive intracranial monitoring. Patients with mild TBI are often seen in the emergency room setting or by the primary care physicians and frequently return home directly after the injury. They usually do not require inpatient hospitalization and no consistent medical treatment for the consequences of mild TBI are employed currently. (Comper P, 2005)

Immediately after an impact injury to the cranium, athletes and soldiers can be significantly disabled. Fine motor skills and balance are acutely affected, creating a situation where the patient can have severe impairments of motor and executive judgment that can expose themselves and others to further harm. Long-term consequences include pain syndromes, such as chronic headaches, nausea and visual disturbances. Patients may also experience difficulties with cognitive tasks, such as learning disability, difficulty with concentration, and short-term memory loss. Further, long-term neuropsychological disabilities from TBI include mood instability and derangements of perception. (Hogue C, 2008).

1.3 Pathophysiology of Traumatic Brain Injury

As stated previously TBI can broadly be categorized as penetrating or non-penetrating injuries. Non-penetrating injuries occur when the brain moves inside the skull striking the inner surface of the skull, movement of the brain against the rigid bone causes mostly focal injuries to the frontal and temporal poles of both hemispheres. (Bruns J, 2003)

Non-penetrating injuries include those caused by inertial forces: linear translation or rotation combine to produce angular acceleration and deceleration that cause shearing and normal forces that damage large numbers of neural masses. The forces are greatest in areas that experience the highest angular acceleration (superficial>deep and anterior>posterior). Shearing forces are maximal between tissues of different densities such as the interface between the gray and white matter. At a mesoscopic scale (1mm range), high velocity and long-duration acceleration are maximal on axonal projections and small blood vessels causing shearing of axons and disconnections of synapses.

The cellular response to TBI has been investigated in animal models that involve studying brain tissue after a mass has impacted a surgically opened area of brain (Cernak, 2005) It is hypothesized that a mechanical strain and tearing results in mechano-poration of the cell membrane and axon, causing a massive release of intracellular contents including excitatory

neurotransmitters and intracellular ions. The most readily observed changes after traumatic injury include the release glutamate and calcium ion into the extracellular space. (McAllister, 2011)

Cells that are entirely disrupted undergo necrosis in the minutes after injury and trigger an inflammatory response. In surrounding cells with damaged plasma membranes, the influx of Ca^{+2} into the cell sets off an intracellular cascade that leads to cytotoxic damage. In certain cases, cells that are relatively less severely injured can undergo programmed cell death in the hours to weeks after the injury. However, the effect of mild injury has not been well described. The excessive release of other neurotransmitters can further electrophysiological derangements after trauma. Acetylcholine, may amplify the destruction of excitatory amino acids. Serotonin elevations can decrease cerebral glucose use and lead to further metabolic derangements. (McAllister, 2011)

1.4 Biomarkers of TBI

Current biomarkers to predict the outcome of TBI depend on clinical assessments obtained at the time of injury; specifically the Glascow Coma Scale mentioned in an earlier section. Other tests of concussion consist of neuropsychological examinations such as the ImPACT (impacttest.com) (McClincy M, 2006) or the ANAM military TBI assessment (Irvins BJ, 2009). None of these clinically based indicators are very accurate at predicting neurological deterioration, nor are reliable to aid in prognosis or treatment response.

Traditional imaging techniques, such as CT and MRI scans, can visualize gross changes in neuroanatomical structure such as skull fractures and brain hemorrhages. However, individual cellular injury cannot be easily discerned from these images, much less the damage to the underlying neural networks that are the cause of the spectrum of clinical presentations of traumatic brain injury. Some functional magnetic resonance imaging (fMRI) studies into TBI have been conducted but are expensive and not easily useable to monitor function continuously (Friedman SD, 1999)

Since the brain is an electro-dynamical system, it creates electric fields indicating internal activity that may be recorded at the scalp by way of electroencephalography (EEG). Hans Berger first discussed the use of EEG in humans. (Berger, 1969) EEG can be used to monitor the electrical activity of the normal and diseased brain in a variety of conditions. EEG has been used after moderate and severe traumatic brain injury to monitor for subclinical seizures and is being actively pursued as a valuable measure of the treatment response in acutely injured patients. Due the fact that it is a passive sensor, EEG can be used continuously, is safe, non-invasive and relatively inexpensive. Our aim is to design a computational model that can utilize EEG to monitor the electro-dynamic changes that occur after TBI as a biomarker of disease progression, treatment response, and prognosis.

2 Computational models of TBI

Previous simulation endeavors into TBI have focused on finite element modeling of mechanical stress and strain relationships to describe the deformation of neural structures after various head impacts (King AI, 1995). These modeling efforts did not consider the changes to the underlying electrodynamics that occurs after TBI. Computational modeling of TBI has also included modeling changes to cognitive processes after TBI in an effort to describe the alterations in cognitive processing by varying the values of different judgment functions. There have been multiple efforts to model the neurophysiological changes that occur with epilepsy syndromes using computational models (Knowles, 1985).

There are no current computational models of electrodynamics of the neural systems under various traumatic injury conditions. This paper formulates such an approach to model the electrodynamics of brain injuries based on lumped neural mass models. The objective is to create an electrodynamic model that captures the macroscopic response, at the level of EEG recordings, of the brain to various injury conditions. Following previous research efforts by Ursino (Ursino M, 2010) and Bhattacharya (Bhattacharya BS, 2011) the present study focuses on the frequency domain behavior of the brain electrodynamics after TBI.

3 Neural Mass Models

Various mathematical models of the brain have been proposed in the past several years. These range from single spiking neuron models capturing membrane dynamics and chemical transport phenomena, to population models that capture the average behavior of densely connected mass of neurons. Although incapable of predicting the responses of individual neurons, these latter models are useful in characterizing the macroscopic electrodynamics of the brain, observable from external measurements such as the EEG.

Neural Mass Models (NMM) are used in the present study for modeling populations of neurons in the cortex. Since the introduction of the NMMs by Wilson and Cowan(Wilson HR, 1972) they have been widely used in a range of modeling efforts. Briefly, in these models, a population of neurons is assumed to have a shared input and output connectivity. Further, spiking activity is modeled for a coalesced population soma rather than individual neurons. The underlying assumption is that as long as the population neurons are connected to each other (either directly or via local interneurons) the spatial interactions can be neglected in favor of temporal dynamics of the aggregate population. This approach is justified as there is a high degree of local redundancy in cortical tissues. In other words, many neighboring populations exhibit similar response to identical stimuli. Thus, rather than attempting to duplicate a higher level function through detailed model of individual neurons and their connectivity, NMM's offer a macroscopic view of the temporal dynamics of populations of neurons. This macroscopic view can be useful in analysis of higher level global processes such as pattern recognition. Further, while individual neuron's activity may appear random, a macroscopic view of the neural population may yield precise interactions over larger scales. The NMM representation is mathematically tractable and parsimonious, since only a few variables are needed in the model to capture the dynamics of a population of neurons.

The original NMMs modeled both excitatory and inhibitory neural sub-populations. These were adapted to reproduce various rhythms associated with the neural activity of the brain using feedback loops amongst various populations. For example, Lopes da Silva, et. al. have modeled the alpha rhythms and other rhythms (Lopes da Silva FH, 1976). Recently, Bhattacharya (Bhattacharya BS, 2011) used a neural mass model to approximate the effects of Alzheimer's disease as a global loss of neurons.

In the present project, two different NMMs are simulated following previous research. The first model is based on a paper by Jensen and Rit (Jansen BH, 1995)that uses biologically feasible values to simulate connectivity between two cortical columns1. The second model, is from Ursino et. al (Ursino M, 2010) this work is one of the most sophisticated models available and allows for simultaneous alpha and gamma rhythm generation. In the next sections, we describe the details of these models and their application to TBI.

4 Model 1: Jensen and Rit Model for a Cortical Column

[11] This work is highly cited, and is reproducible in comparison to the models employed in some newer papers that were examined at the start of the present project.

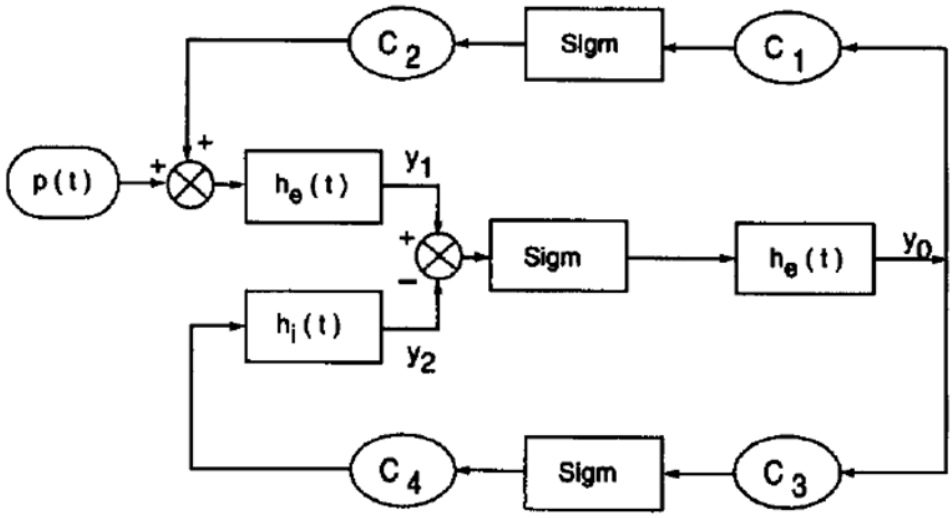

Figure 1. The Jensen-Rit Neural Mass Model

Figure 2 shows a NMM for a cortical column used for generation of alpha rhythm. The model uses 3 neural sub-populations each with a post-synaptic potential (PSP) block that converts pulse density into potential and a sigmoid block that converts potential into pulse density. The constants C1, C2, C3, and C4 are the connectivity constants that define synaptic connectivity of the interneurons between different subpopulations. The PSP blocks hi (inhibitory interneuron) and he (excitatory interneurons and pyramidal neurons) represent linear transformations that are defined by the following impulse responses:

$$h_e(t) = Aate^{-at}, t > 0, 0\ otherwise$$
$$h_i(t) = Bate^{-bt}, t > 0, 0\ otherwise$$

Here, A and B are the gain, and a and b are the lumped representation of the sum of reciprocals of the time constants of the associated delays.

The sigmoidal functions in the model are defined as

$$Sig(v) = 2e_0/[1 + e^{r*(v_0 - v)}]$$

Here, $2e_0$ is the maximum firing rate, v_0 is the firing threshold and r determines the steepness of the sigmoid. The model also accounts for input from other cortical areas. These are modeled as white noise with a uniformly distributed amplification factor.

A Simulink® implementation of the Jensen-Rit model for a cortical column in the visual cortex[2] is given in Figure 3. Simulation of the visual cortex was chosen for this initial implementation due to the fact the frontal lobe and occipital lobes are both vulnerable in TBI and visual disturbances are common after TBI (Hardman JM, 2001) The alpha frequency is prominent in the occipital lobe when the eyes are closed and the subject is at rest. (Romei V, 2010)

[2] The model parameters change for other cortex.

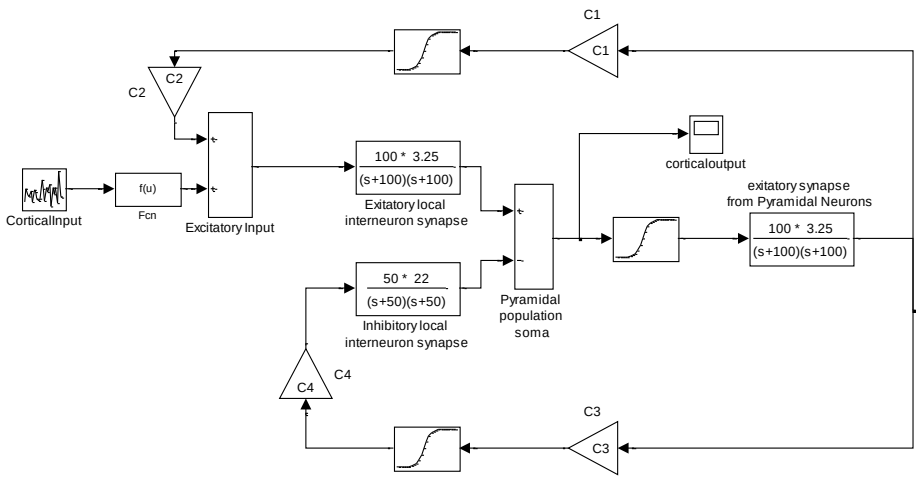

Figure 4. Simulink Block Diagram of the Jensen-Rit Visual Cortex Model

The potential of the neural mass soma is plotted in Figure 3. Notice that the temporal evolution of the membrane potential exhibits oscillations.

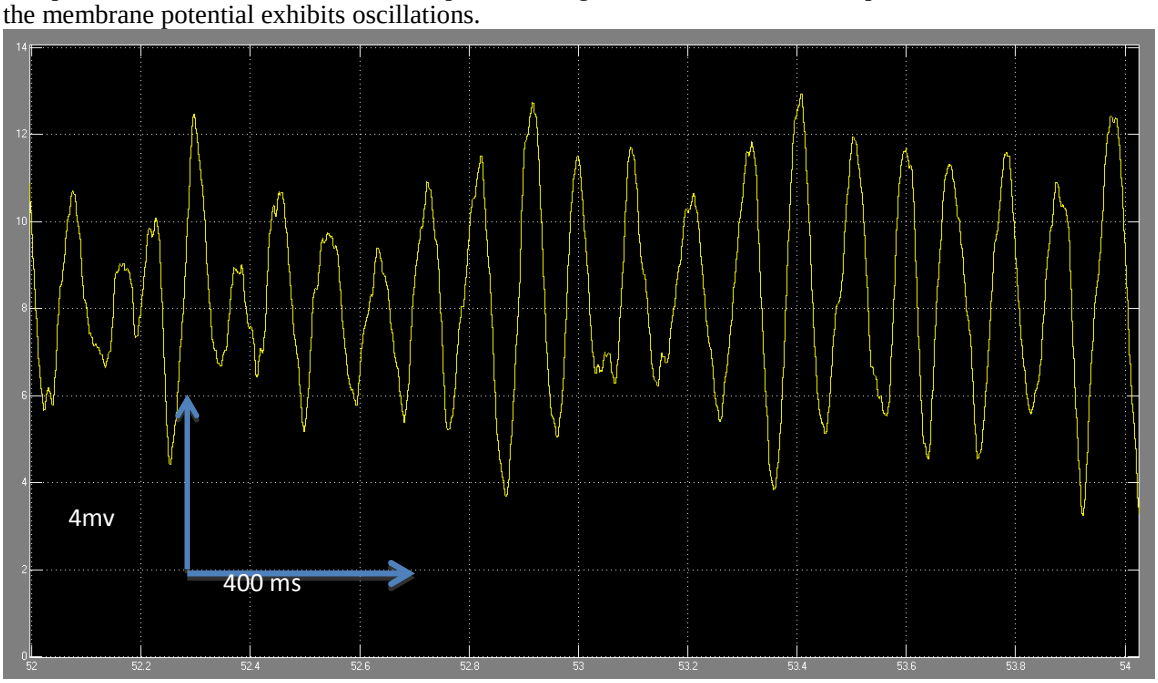

Figure 3 Oscillations in membrane potential of pyramidal cell soma

The normalized power spectral density (i.e. PSD(f)/∑PSD(f)) of the membrane potential history is given in Figure 6.

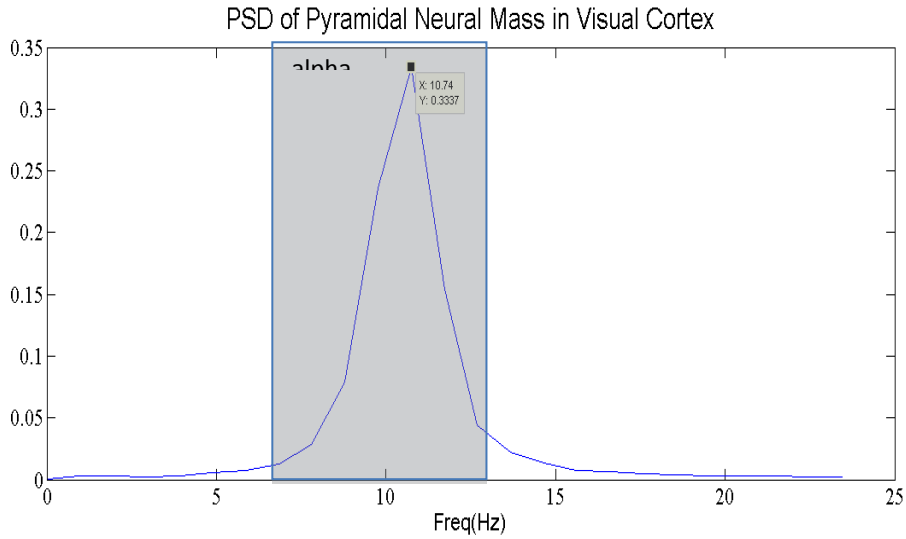

Figure 6. Normalized Power Spectral Density of the Jensen-Rit Visual Cortex Model

Figure 6 shows that the alpha band frequencies (8-12Hz) are the dominant frequencies in the visual cortex model and therefore accurately simulates an awake, resting patient with his eyes closed.

4.1 Modeling a mild TBI using Jensen-Rit model

During a mild TBI, the potassium and calcium influx cause a temporary increase in the spiking activity. This is modeled in the present work by reducing the firing threshold in the sigmoid function for the pyramidal neurons. Since layer V of the cortical mantle is most at risk during mild ischemic injuries, we assume that the pyramidal neurons are most likely to sustain damage during mild non-penetrating TBI. (Kandel ER, 2000)

The effect of lowering of the firing threshold of pyramidal neurons in mild TBI is illustrated in Figure 7.

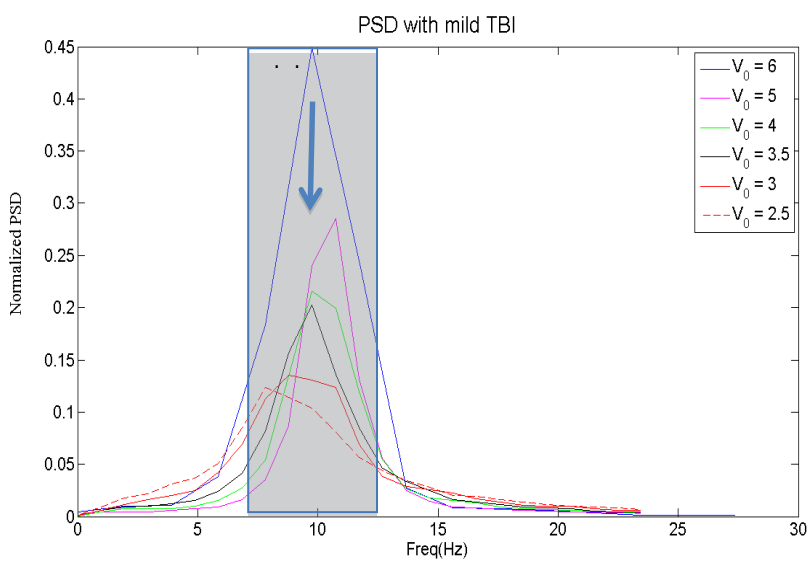

Figure 7. The Effect of Lowered Firing Threshold of Pyramidal Neurons in Mild TBI

The following observations can be made from Figure 7.

Overall contribution of alpha band to PSD reduces monotonically with the threshold. The peak observed in the alpha band is lowered in magnitude as the threshold potential is reduced. The PSD is more dispersed. Although a slight decrease in threshold appears to cause the peak in the alpha band to move to the right (i.e. towards higher frequencies), it can be observed that further decrease moves the peak towards the left.

Thus, noting the above patterns, it may be possible to design appropriate EEG markers for mild TBI. A good marker for TBI may use the total contribution of alpha band as well as the location of peaks in the power spectrum to determine the magnitude of a TBI.

4.2 Modeling moderate TBI

A moderate TBI can be modeled as a loss in synaptic connectivity due to injuries to small focal areas of the brain. Figure 8 shows that reduced synaptic connectivity (20% loss) causes the peak band to shift from alpha (8-12Hz) to lower frequency delta rhythms (0.1-4Hz).

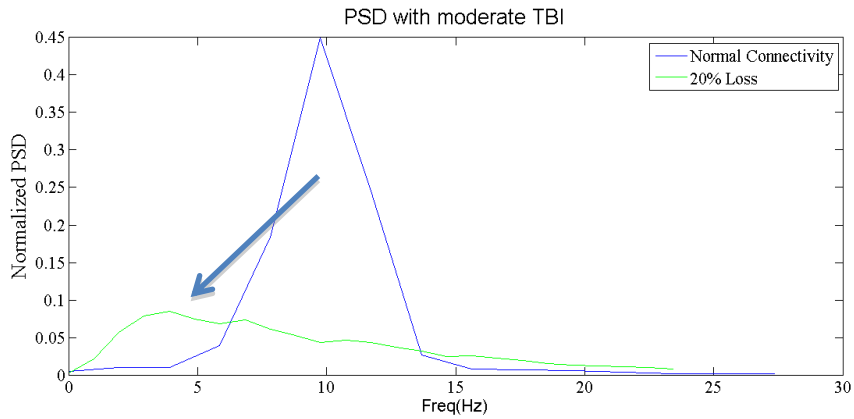

Figure 8. Shift of Power from alpha (8-12Hz) to Lower Frequency Delta Rhythms (0.1-4Hz) due to Reduced Synaptic Connectivity in Moderate TBI

Next, a loss of synaptic connectivity to only the pyramidal neurons is evaluated. A mild TBI is also included in the model by reducing the threshold potential V_0 to 4 mv (from 6 mv). Thus, a combination of injuries (dashed red) and a possible means of recovery (solid red) are both simulated. Notice how the permanent injury of 20% of the neurons (green in Figure 8) closely resembles the temporary injury (dashed red in Figure 9). Thus, temporal progression of EEG rhythms can reveal interesting information on TBI and subsequent recovery.

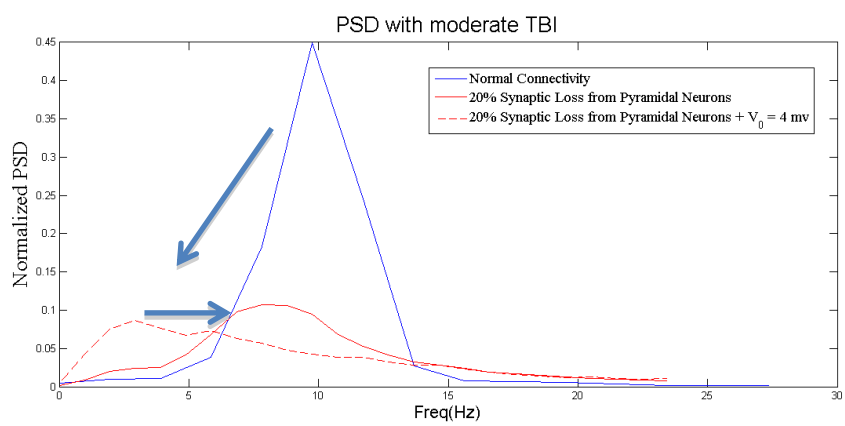

Figure 9. PSD of the NMM with Moderate TBI

4.3 Connected Cortical Columns

As shown in the schematic diagram below, the Jensen and Rit model also allows for connecting multiple cortical columns using attenuation and delay.

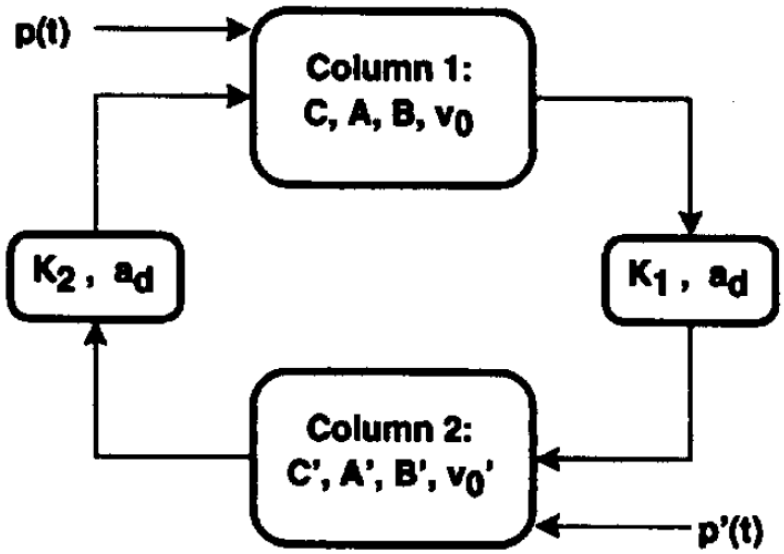

Figure 10 Two Connected Columns using Jensen and Rit model

Since, the primary focus of the present study is on a localized injury, two neighboring cortical columns from the same (occipital) cortex were connected together.

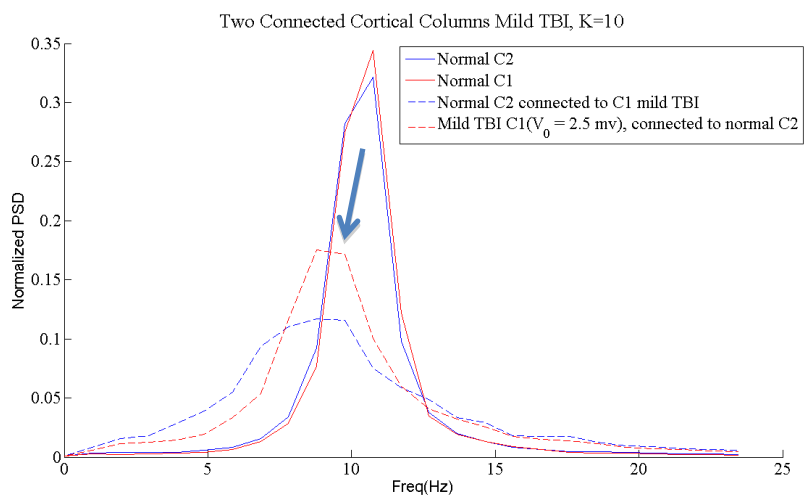

Figure 11. PSD of two connected cortical columns

Figure 11 shows the PSD of two connected cortical columns from the visual cortex (see (Jansen BH, 1995) for details). The "normal" scenario PSD is similar to that shown earlier for the single column. However, when one column undergoes a mild TBI, i.e. firing threshold for pyramidal neuron is lowered to 2.5 mv from 6 mv, it may be observed that the PSD of the membrane potential of the "normal" neighbor also gets smeared (An attenuation factor, or K value, of 10 and a_d = a, i.e. the signal attenuates to $1/10^{th}$ of its value in reaching the neighbor is employed). Note that the observed EEG at any of the electrodes is the weighted sum of rhythmic activity from many different areas, where the weight depends on the spatial distance from the measuring electrode. To see the effect of distance, TBI in coupled neurons that are further apart with a higher attenuation factor (K = 60) are also simulated.

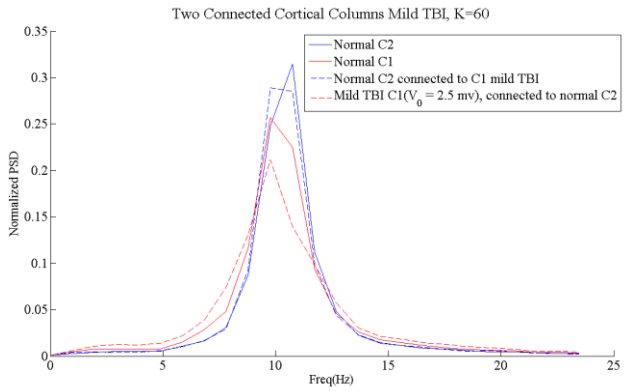

Figure 12. PSD of two connected cortical columns with K=60

It may be observed that the input from a "normal" cortical column ameliorates the PSD to certain extent, i.e. masks the smearing effect observed earlier. However, the "normal" column PSD is not impacted significantly.

In Figure, a mild TBI in neighboring coupled cortical columns is induced. The coupling between columns causes the PSD to be almost identical even with mild TBI, and both columns exhibit the flattening of the PSD.

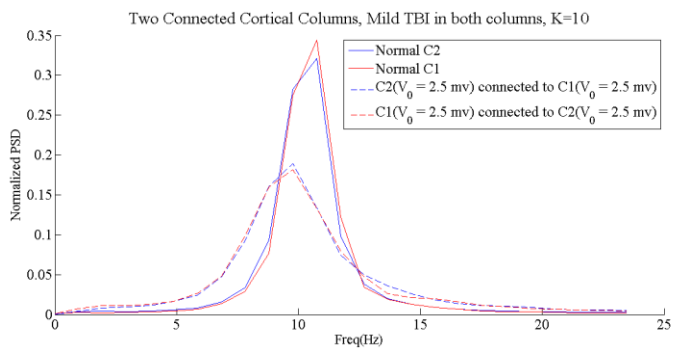

Figure 13. Smearing of the PSD due to mild TBI

Thus, from the above plots, it can be concluded that that a mild TBI to a cortical column can indeed manifest in the electrical activity of its immediate neighbors. Further, as the distance grows and the connectivity between columns is reduced, the effect on neighboring columns is decreased in this model. Even somewhat distant neighboring columns can mask the severity of a mild TBI (reduce the smearing effect on PSD). If the area of a mild TBI encompasses multiple cortical columns, the smearing of the PSD can be useful marker in determining the location and spatial extent of the injury.

The above results can be used for creating an EEG marker for mild TBI in terms of magnitude and location of the injury. Such precise information can be very useful in determining the recovery measures.

5 Model 2: The Ursino Neural Mass Model

The Ursino model improves upon the Jansen & Rit model discussed in the foregoing sections by adding a fast inhibitory interneuron loop. This loop plays a significant role in the generation of γ-band oscillations. These gamma frequencies are important for attention and concentration tasks performed by the frontal lobe (Gaona, 2011) and may provide a good biomarker for TBI, since difficulties with cognitive tasks such as impaired concentration are a hallmark of TBI.

In order to model a whole cortical area the four populations – excitatory, fast and slow inhibitory interneuron, pyramidal neurons – are connected via excitatory and inhibitory synapses with impulse responses $h_e(t)$, $h_f(t)$ and $h_f(t)$. The average numbers of synaptic contacts among neural population are represented by eight parameters C_{ij}, where the first subscript represents the target (post-synaptic) population and second subscript denotes the pre-synaptic population. These are illustrated in Figure 12.

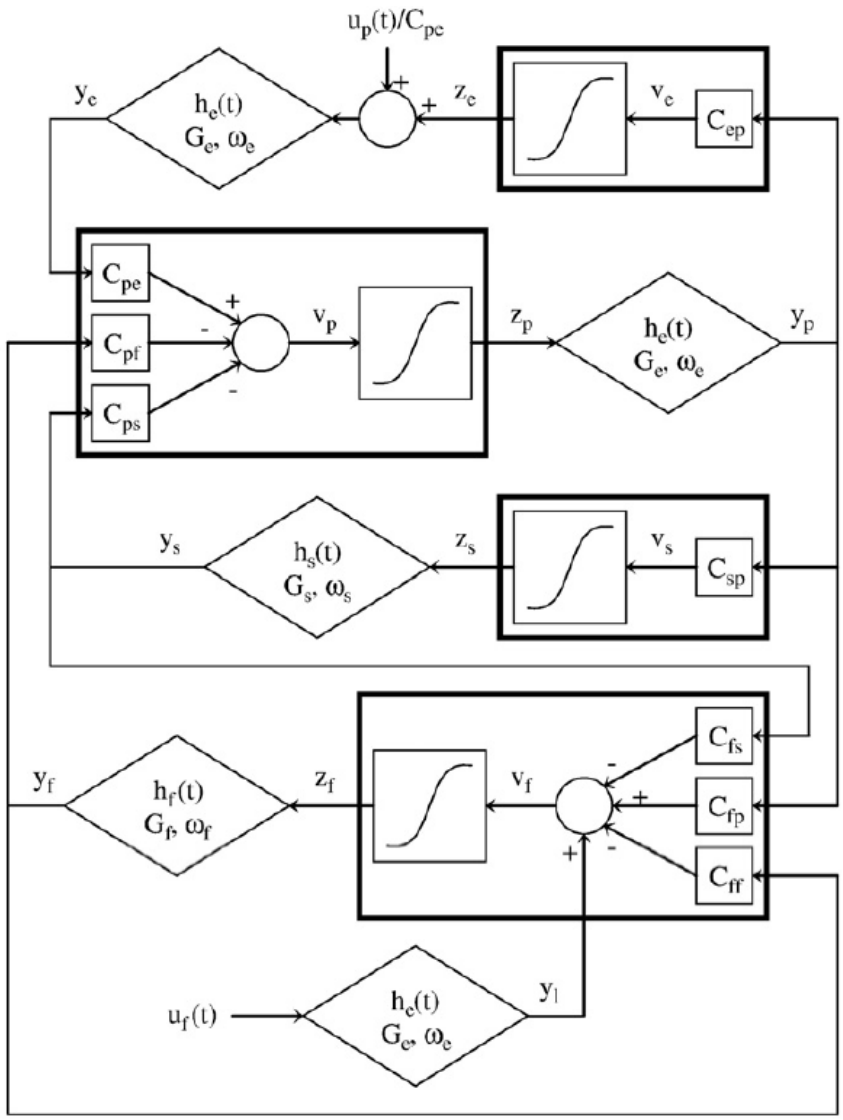

Figure 14 Single Cortex model as proposed by Ursino

An important aspect of the model is that it explicitly includes external inputs. Since inputs originate from pyramidal neurons in other cortical areas, this model assumes that they always act via the excitatory synapses. Lateral connections in the cortex target all layers, and hence, the inputs can reach pyramidal cells, excitatory interneurons as well as inhibitory interneurons. For brevity, the present model considers only inputs to pyramidal neurons and to fast inhibitory interneurons.

The connectivity between two separate cortical areas is modeled as excitatory connections with a time delay. The average spike density of the pyramidal neurons of the pre-synaptic area (z_p^k) affects the post-synaptic area through a weight factor W_j^{hk}, where j = p or f depending on

whether the synapse target to pyramidal neurons or fast inhibitory neurons and a time delay T. This is achieved by modifying the input quantities u_p^h or/and u_f^h of the target region. This can be expressed mathematically as:

$$u_j^h(t) = n_j^h(t) + W_j^{hk} Z_p^k(t - T) \qquad j = p, f$$

where $n_j(t)$ represents Gaussian white noise.

5.1 Implementation of Single Cortex model

Figure 15 illustrates the single cortex implemented in the present work. It is similar to the previous figure and specifies all the parameters of the model.

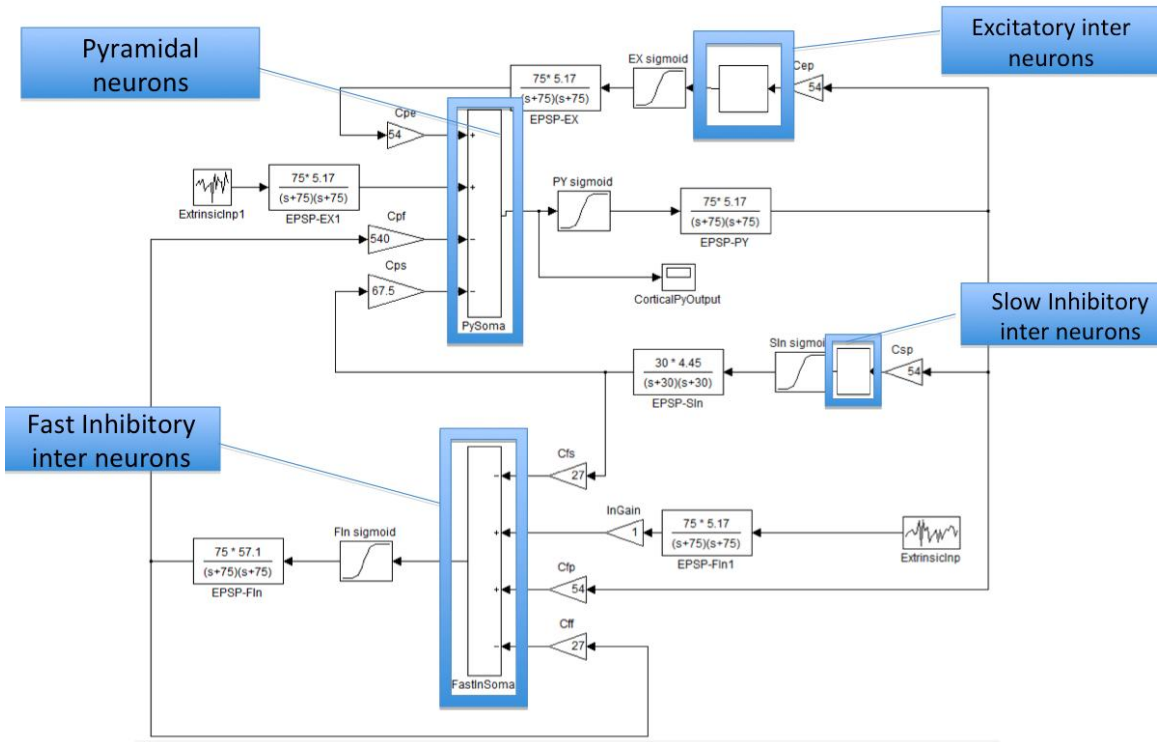

Figure 15 Implementation of Cortex model

The input provided to the model is generated using a white Gaussian noise with mean $m = 0$ and variance $\sigma^2 = 5$. The output and input are sampled at 1000Hz.

Figure 16 illustrates the post-synaptic potential generated at the output of the pyramidal neurons in the model given in Figure 15. As can be observed, it shows oscillations at the low and high frequency band (Figure 15) Figure 16 below represents the EEG of a human recorded from the frontal lobe in a concentration task. The frequency spectrum in Figure 15 is similar to Figure 16 and also shows peaks at the gamma band range.

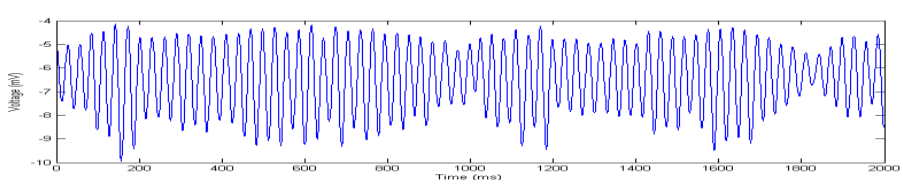

Figure 16 Post-Synaptic potential at Pyramidal Neurons

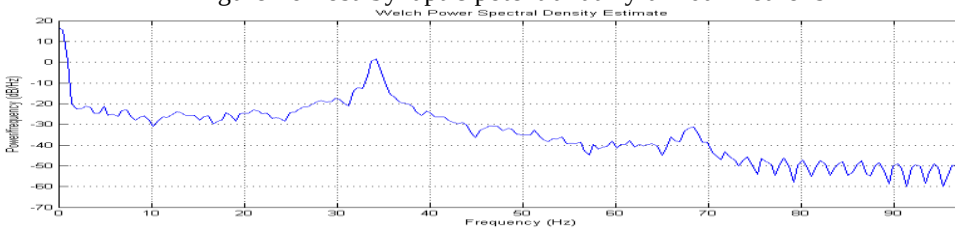

Figure 17 PSD of Post-Synaptic Potential generated by the model

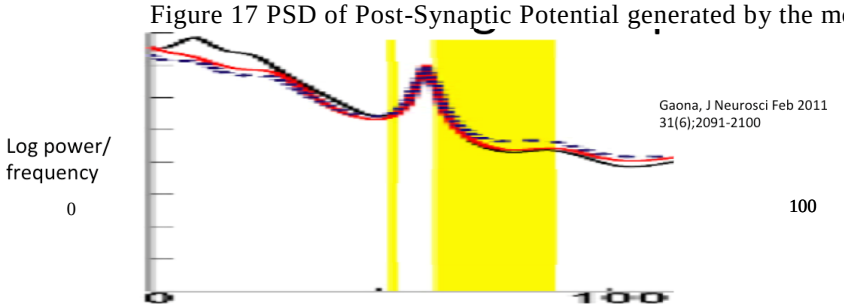

Figure 18 EEG of Human Brain in a concentration task (Gaona, 2011)

5.2 Implementation of A Dual Cortex model

Figure 19 represents two instances of the above cortex models connected through long- range connectivity functions explained before.

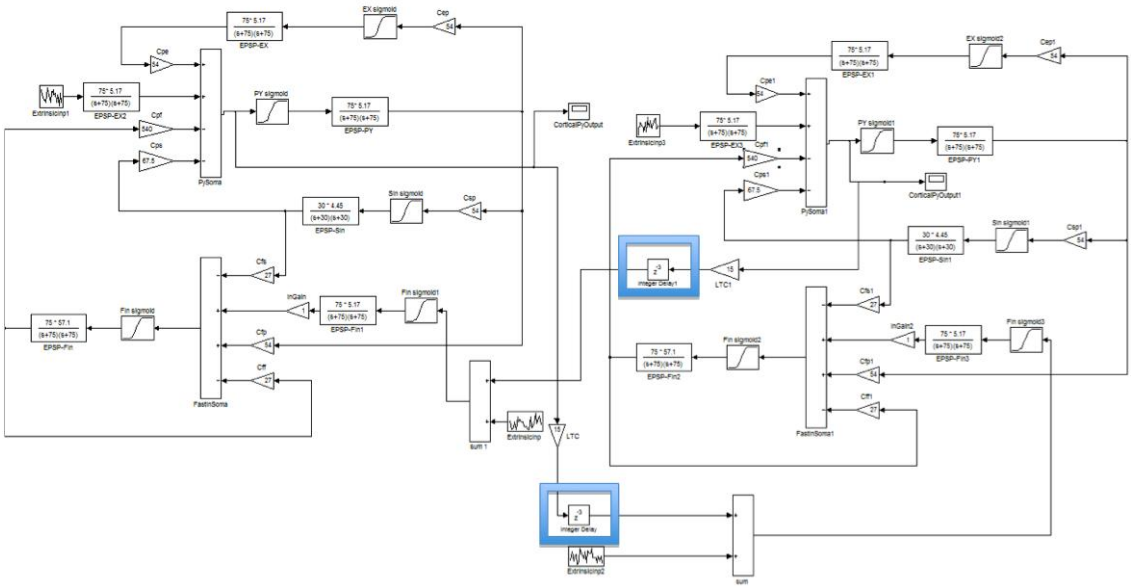

Figure 19 Dual Cortex model

As can be observed from the above figure, the pyramidal population of each model provides inputs to the fast inhibitory interneuron in the other. A time delay of 10ms is used to simulate the delay introduced due to long distance connectivity. The weight of each connection is set at 15.

5.3 Moderate to Severe TBI in Dual Cortex model

In order to simulate moderate to severe TBI in the dual cortex model, effective synaptic connectivity between neural populations (C_{ij}) is reduced in one of the cortex models. The behaviour of the model at various levels of connectivity was measured and is illustrated below.

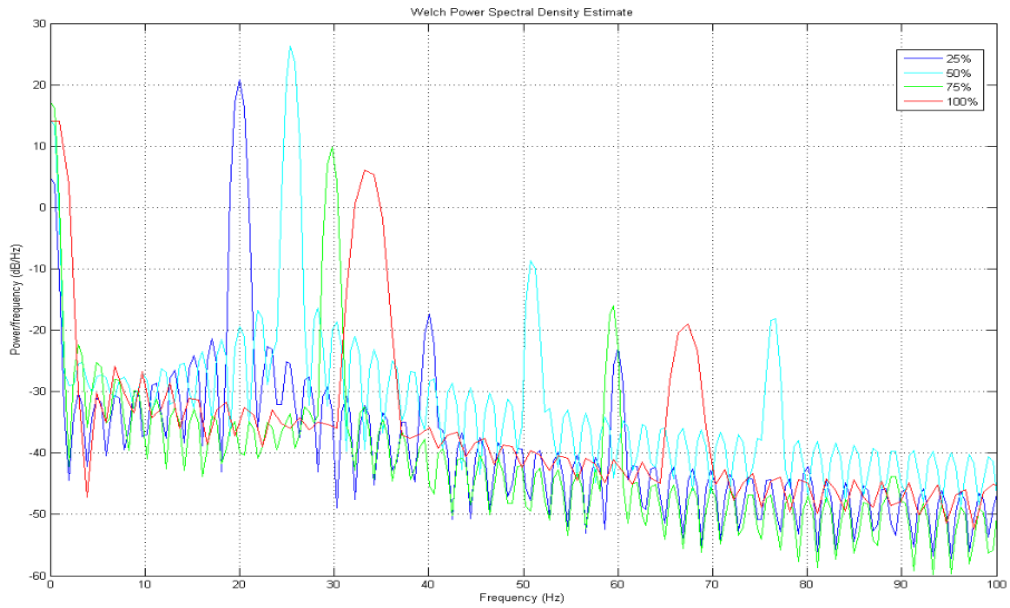

Figure 20 PSD/Frequency at different connectivity levels

As can be seen from the figure above, the peak at 25% connectivity is around 20Hz (blue line) and peak at 100% connectivity is around 34Hz (red line). Thus, as the connectivity decreases, the peak moves towards a lower frequency. This is similar to those observed in moderate brain injuries where diffuse slowing of activity (increased low frequency activity) is a sign of injury.

5.4 Mild TBI in Dual Cortex model

Mild TBI is observed in the initial few moments after an injury to the brain. In a mild TBI, there is an increase in Glutamate which is an excitatory neurotransmitter. This results in an increase in the firing rate of the neurons. This can be modeled by increasing the slope of the sigmoid function. As expected, the peak occurs at a higher frequency with increasing firing rates.

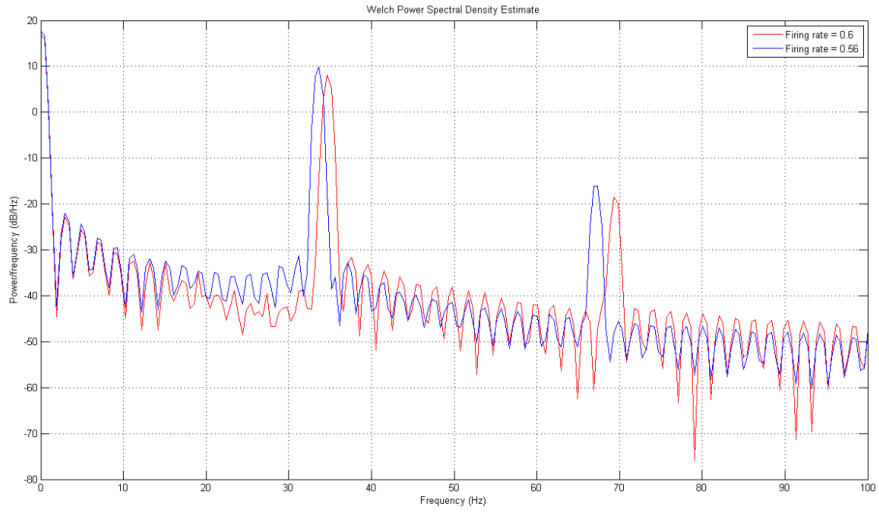

Figure 21 Mild TBI Simulation

4 Summary and Conclusions

This paper presented an investigation into the feasibility of using neural mass models to characterize the macroscopic frequency domain response of the brain to traumatic brain injuries.

Traumatic brain injury is a disease of local damage to local neural masses that create the clinical symptoms discussed in the earlier portions of this paper. There is a pressing need for the development of neurophysiologically based models of the disease to aid in disease monitoring, progression and treatment response.

Basic single and dual cortex architecture models were developed during the present study. Gaussian white noise excitation, simulating the resting brain was used to analyze the dominant frequency components in the spectrum of the model response. It was then demonstrated that the present model accurately captures the alpha and gamma rhythms observed in the EEG of resting brain. TBI was simulated by varying the neural mass connection parameters in the model. Simulated moderate and severe TBI create changes in the power spectral density of the model outputs that begin to approximate observed clinical changes. A marker of mild TBI is described based upon well-described physiological derangements after concussions. Using the Jansen and Rit model, the changes to the alpha band in the occipital lobe after various traumatic injuries was demonstrated, and possible mechanisms of recovery was advanced. Moreover, changes to the gamma band of the frontal lobe after various injuries were demonstrated using the Ursino neural mass model.

The highly positive nature of present work motivates future explorations into the design of graduated animal experiments to describe neurophysiological changes associated with TBI.

Future work will also undertake a more thorough linear analysis of a dual cortex and multicortex model to supplement the simulation results. These investigations will allow more accurate prediction of changes to brain's electrodynamic activities due to TBI and will aid in the reconstruction of clinically derived EEG recordings. Other future research directions can include creating an EEG shell model employing several more interconnected neural mass models to simulate other traumatic injury scenarios and create the associated scalp EEG readings that can be used to correlate with clinically derived EEG recordings (see appendix for an initial Simulink® model) .

Bibliography

Berger, H. (1969). On the electrocencephalogram of man. *Electroencepahlogr Clin Neurophysiol* (Suppl 28:37).

Bhattacharya BS, C. D. (2011). A thalamo-cortical-thalamic neural mass model to study alpha rhythms in Alzheimer's disease. *Neural Networks , 24*, 631-645.

Bruns J, H. W. (2003). The epidemiology of traumatic brain injury: a review. *Epilepsia , 44(suppl10)*, 2-10.

Cernak, I. (2005). Animal models of head trauma. *NeuroRx , 3*, 410-422.

Comper P, B. S. (2005). A systematic review of treatments for mild traumatic brain injury. *Brain Injury , 19* (11), 863-880.

Friedman SD, B. W. (1999). Quantitative proton MRS predicts outcome after traumatic brain injury. *Neurology , 52* (7), 1384-1391.

Gaona, C. S. (2011). Nonuniform high-gamma (60-500hz) power changes dissociate cognitive task and anatomy in human corte. *J of Neuroscience , 6*, 2091-2100.

Hardman JM, M. A. (2001). Pathology of head trauma. *Neuroimaging Clin North Am , 2*, 175-187.

Hogue C, M. D. (2008). Mild traumatic brain injury in US soldiers returning from Iraq. *New England Journal of Medicine* (385), 435-463.

Irvins BJ, K. R. (2009). Performance on the automated neuropsychological assessments metrics (ANAM) in nonclinical sample of soldiers screened for mild TBI after returning from Iraq and Afghanistan: a descriptive analysis. *Journal of Head Trauma Rehabilitation , 1*, 24-31.

Jansen BH, R. V. (1995). Electroencephalogram and visual evoked potential generation in a mathematical model of coupled cortical columnns. *Biol Cybern , 73*, 357-366.

King AI, R. J. (1995). Recent advances in biomechanics of brain injury: a review. *J Neurotrans , 4*, 651-8.

Knowles, W. (1985). Properties of neural networks: experimentation and modeling of the epileptic hippocampal slice. *TINS , 8*, 73-79.

Lopes da Silva FH, R. A. (1976). Model of neuronal populations:the basic mechanism of rhythmicity. *Prog Brain Res , 45*, 281-308.

McAllister, T. (2011). Neurobiological consequences of traumatic brain injury. *Dialogues Clinical Neurosciences , 13*, 287-300.

McClincy M, L. M. (2006). Recovery from sports conucssion in high school and collegiate atheletes. *Brain Injury , 1*, 33-39.

Rabenstein. (2008). Principles of Neurointensive care: Chapter 49. In Bradley, *Neurology in Clinical practice 5th edition.* Philadelphia, PA: Butterworth-Heinemann Elsevier.

Rigg JL, M. S. (2011). Concussions and the miliary: issues specific to service members. *PM&R Concussion and Mild TBI: Current and future concepts , 3* (10), S380-S386.

Romei V, G. J. (2010). On the role of prestimulus alpha rhythms over occipitio-parietal area in visual input regulation: correlation or causation? *J Neurosci , 25*, 8692-7.

Teasdale G, J. B. (1974). Assessment of coma and impaired consciousness. A practical scale. *Lancet* , 81-4.

Tisdall MM, S. M. (2006). Cerebral microdialsys:research technique or clinical tool. *British J of Anesth , 1*, 18-25.

Ursino M, C. F. (2010). The generation of rhythms within a cortical region:Analysis of a neural mass model. *NeuroImage , 52*, 1080-1094.

Wilson HR, C. J. (1972). Excitatory and inhibitory interactions in localized populations of model neurons. *Biophysical journal , 12*, 1-24.

Appendix

We implemented a model for multiple connected columns, such that each column is connected to its 4 neighbors. To avoid egde effects, the columns on the top row are connected to the bottom row and the ones on the left to the right. Then we create a TBI in the central node and observe the PSD changes in the grid.

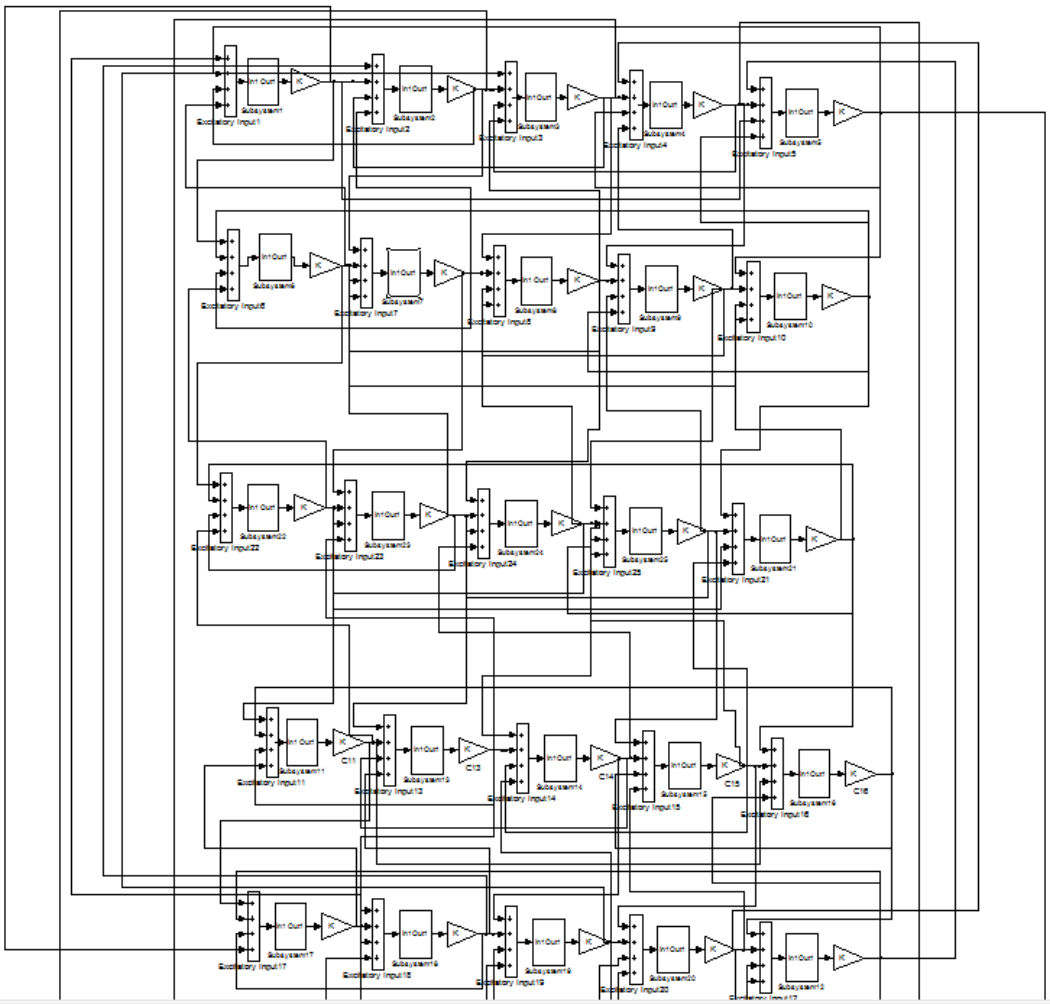

Multiple Cortical column model